Universiteit
Leiden
The Netherlands

Approaches to structure and dynamics of biological systems by electron-paramagnetic-resonance spectroscopy

Scarpelli, F.

Citation

Scarpelli, F. (2009, October 28). *Approaches to structure and dynamics of biological systems by electron-paramagnetic-resonance spectroscopy*. *Casimir PhD Series*. Retrieved from https://hdl.handle.net/1887/14261

Version:	Corrected Publisher's Version
License:	Licence agreement concerning inclusion of doctoral thesis in the Institutional Repository of the University of Leiden
Downloaded from:	https://hdl.handle.net/1887/14261

Note: To cite this publication please use the final published version (if applicable).

Chapter 4. Aggregation of transmembrane peptides studied by spin-label EPR

4.1 Introduction

The assembly and folding of membrane proteins, and the association of these proteins inside the membrane depend strongly on the balance between protein-protein and protein-lipid interactions. Peptides forming transmembrane (TM) α-helices and their interactions with phospholipid bilayers serve as models to define the elementary aspects of the protein-membrane interactions governing the properties of TM proteins (Fig. 1a). The WALP peptide (Acetyl-GWWL$(AL)_n$WWA-amide) is one of the paradigmatic TM peptides and its properties have been studied in various membrane environments. [2-6]

The response of peptides and ultimately membrane proteins to changes in membrane conditions depends on the balance of peptide-peptide, peptide-lipid and lipid-lipid interactions. Consequently, the type of lipid (saturated vs unsaturated) and the membrane phase (gel phase vs. liquid-crystalline phase) are important factors. One of the intriguing and potentially biologically relevant responses of the peptides to different membrane conditions is aggregation. Since membrane systems are intrinsically disordered and dynamic, many conventional methods for structure investigation cannot be employed to monitor peptide aggregation. Also, often these methods can only probe aggregation in certain lipids or phases of the membrane, for example, because the phase of interest occurs in an inaccessible temperature range. Thus, a combination of methods is needed to address the question of how the balance of forces in peptide-membrane interactions does influence peptide aggregation.

For WALP peptides it has been shown by atomic force microscopy (AFM) and fluorescence techniques, that they form linear aggregates in the gel-phase of a saturated lipid (DPPC).[1,7,8] In the liquid-crystalline phase of the same lipid, the AFM signatures of aggregation disappear and excimer fluorescence is strongly reduced.[1,8] Also, in the liquid-crystalline phase of an unsaturated lipid (DOPC) a low level of

aggregation was detected by fluorescence.[9] However, aggregation in the gel phase of DOPC has not been investigated.
Here we present spin-label EPR to probe peptide-membrane interactions in relation to peptide aggregation. We show that it is applicable to different lipid systems over a wide temperature range, including low temperatures where also unsaturated lipids form a gel-phase. Spin-label EPR has been used in different ways to investigate membrane-peptide systems,[6,10,11] but the present approach is novel in that the peptide-peptide interaction is directly probed by spin-labeling the peptide in combination with diamagnetic dilution of the samples.

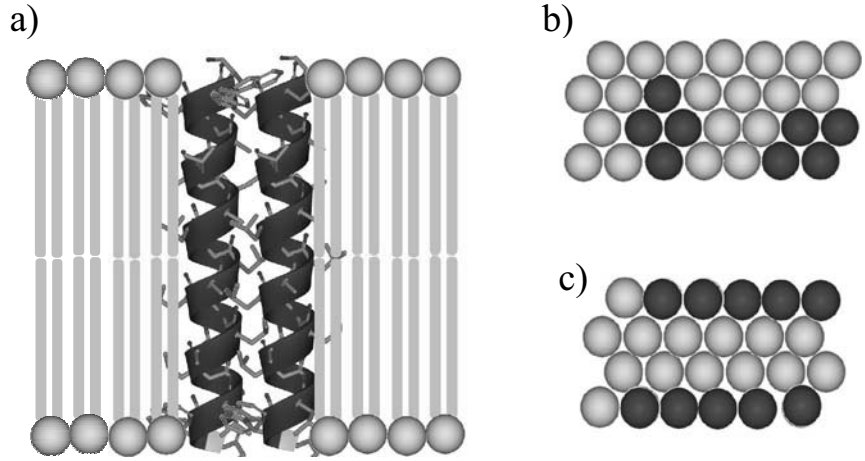

Fig. 1: Schematic representation of WALP peptides in a gel-phase lipid bilayer. (a) Lipid bilayer, lipid head groups (gray), lipid chains, WALP helices, side view. (b) Peptide cluster aggregates, top view. (c) Peptide linear aggregates, top view.

Diamagnetic dilution is an approach that has previously been used to avoid line broadening by spin-spin interactions.[12,13] Here we used it for the following reason. In aggregates, the short distances between the spin labels due to the close approach of the peptides cause characteristic changes in the EPR spectra that serve as an observable for aggregation under the membrane condition in question. Because different membrane conditions by themselves also can result in different spectral properties

of the spin label, one needs to be able to distinguish these effects from the spin-spin interaction caused by aggregation. In diamagnetically diluted samples, the spin-labeled peptide is diluted by an excess of unlabelled peptide while all other parameters, i.e. the temperature, the type of lipid, and the total lipid-peptide ratio, are kept the same. Thus, aggregation can be detected simply as the spectral difference between samples containing labeled peptide only and diamagnetically diluted samples.

Here, the interaction of WALP23 (WALP), where 23 indicates the number of residues, with the liquid-crystalline phases and the gel phases of two lipids, DPPC and DOPC, is investigated. The spin label is introduced at a central position[14] of WALP that is within the membrane (SL-WALP) or close to the N- or C-terminal end of WALP (SL-N-WALP or SL-C-WALP). The sequences of these peptides are given in Table 1.

Table 1

Peptides and their amino acidic sequences

peptide	amino acidic sequence
WALP23	Ac-GWWLALALALALALALALALWWA-NH_2
C(N)-WALP	Ac-CGWWLALALALALALALALALWWA-NH_2
C(C)-WALP	Ac-GWWLALALALALALALALALWWC-NH_2
C12-WALP	Ac-GWWLALALALACALALALALWWA-NH_2

Similar to previous studies,[1,7,8] we find that WALP aggregates in the gel-phase of the saturated lipid DPPC. At the measurement temperature of 120 K, cluster aggregates prevail, with no apparent preference for parallel or anti-parallel arrangement, whereas other studies, performed at higher temperature, indicated a preference for anti-parallel

aggregates.[1,9,14] We hypothesize that at the lower temperature lipid-lipid interactions are stronger than at 297 K, causing the transition from antiparallel line aggregates to cluster aggregates. We also monitored WALP aggregation for the first time in the gel phase of DOPC and found that aggregation is less extensive than in DPPC. These studies allow us to discriminate between the contributions of specific membrane properties, like the phase of the lipids or the saturation of the lipid fatty acid chains, to peptide aggregation.

4.2 Materials and Methods

4.2.1 Sample preparation

The lipids DOPC (1,2-dioleoyl-*sn*-glycero-3-phosphocholine) and DPPC (1,2-dipalmitoyl-*sn*-glycero-3-phosphocholine) were purchased from Avanti Polar Lipids (Birmingham, AL) and used without further purification.
The spin label reagent, methanethiosulfonate-(1-oxyl-2,2,5,5-tetramethylpyrroline-Δ3-methyl) (MTSL), was purchased from Toronto research chemicals (North York, ON). The reagents used for the synthesis and labeling of the peptides were obtained from commercial sources.
The peptides WALP23, C(N)-WALP and C(C)-WALP (table 1) were synthesized as described previously.[1] The peptide C12-WALP (table 1) was synthesized manually, using the same synthesis protocol.
The MTSL label was attached to all three cysteine-containing peptides via a disulfide bridge. A typical labeling experiment proceeded as follows: A clear solution of 10 μmol (~25 mg) C(N)-, C(C)- or C12-WALP in 2.5 ml trifluoroethanol (TFE) was purged with N_2 for 5 min. While keeping the solution under N_2-atmosphere, 10 μl of triethylamine and a N_2-purged solution of 12.5 μmol (3.3 mg) MTSL in 1 ml TFE were added. The reaction mixture was stirred for 48 hr at 4°C and in the dark. The labeled peptides, SL-N-WALP, SL-C-WALP and SL-WALP, were precipitated in cold tert-butyl methyl ether/n-hexane (1:1) and lyophilized from tert-butanol/water (1:1) and obtained in yields of at least 72%.

The peptides were characterized by MALDI-ToF (Kratos Axima, ACTH (18-39) external standard, α-cyano-4-hydroxycinnamic acid matrix) and electro-spray ionization mass spectrometry (ESI-MS, Finnigan LCQ DecaXP Max mass spectrometer operating in positive-ionization mode). The relative intensities of the peaks were not influenced by increased ionization efficiency due to the label, as checked by comparison of mass spectra of (mixtures of) labeled and unlabeled peptides.
In all labeling experiments only the mass of the labeled WALP (Na^+-ionized form) was found: SL-C-WALP; calculated: $[M+H]^+_{ave}$ 2793.53, found: $[M+Na]^+_{ave}$ 2815.27. SL-N-WALP; calculated: $[M+H]^+_{ave}$ 2807.55, found: $[M+Na]^+_{ave}$ 2829.19. SL-WALP; calculated: $[M+H]^+_{ave}$ 2697.36, found: $[M+Na]^+_{ave}$ 2719.48, $[M+K]^+_{ave}$ 2735.46. Based on these results the labeling-efficiency was estimated to be at least 90%.
The samples preparation procedure is described in reference [10] and the lyophilized WALP was dissolved in TFE. The concentration of this stock solution was determined by the absorbance of the tryptophan (trp) at 280 nm using an extinction coefficient of 22400 M^{-1} cm^{-1}. The desired amount of WALP stock solution was transferred into a glass vial and the TFE was evaporated by a nitrogen gas stream. The resulting peptide film was re-dissolved in 50 µl of TFE. This step was repeated one more time. Finally, the peptide film was dissolved in 50 µl of TFE and the desired amount of lipids in chloroform was added. The lipid-peptide solution was dried using a nitrogen gas stream followed by vacuum drying overnight. The peptide-lipid film was hydrated in buffer: 50 mM of Tris at pH 7.5 and 100 mM of NaCl. The sample was then subjected to 10 freeze-thaw cycles, using liquid nitrogen and a water bath at 50° C, respectively. The resulting multilamellar vesicles were dispersed by vigorous vortexing before the measurement.
The peptide-lipid ratio (P/L) is given as the molar ratio. Unless otherwise stated the peptide/lipid ratio is 1/100. The concentration of labeled peptides was kept between 100 and 250µM for all measurements, for the measurements at 120 K 20% glycerol was added to obtain a frozen glass. The diamagnetically diluted samples (dd-SL-WALP) contain the same amount of SL-WALP, but additional unlabeled WALP to result in a fraction of 10% or 20% labeled peptides.

4.2.2 EPR experiments

The X-band cw EPR measurements were performed using an ELEXSYS E 680 spectrometer (Bruker, Rheinstetten, GE) equipped with a helium gas-flow cryostat and a rectangular cavity. For the measurements in frozen solution, 4 mm outer diameter quartz sample tubes were used and samples were frozen in liquid nitrogen before inserting them in the pre-cooled helium gas-flow cryostat. The EPR spectra were recorded using a modulation amplitude of 2 G and a microwave attenuation of at least 23 dB. Typical accumulation times have been 28 min.
For measurements in liquid solution, where capillaries of 1.3 mm inner diameter were used, the modulation amplitude was adjusted to avoid lineshape distortions, typical value was 0.4 G. To control the sample temperature during measurements above room temperature a nitrogen gas-flow cryostat was used. The EPR spectra were recorded using a microwave attenuation of 15 dB; the total measurement time was up to 70 minutes.
All spectra were acquired using a modulation frequency of 100 kHz. The spectra were baseline corrected and normalized to the same number of spins.

4.2.3 Simulation of the EPR spectra

The cw EPR solution spectra were simulated using *EasySpin 2.6.0*. [15] For all simulations the following tensor values were used: G = [g_{xx} g_{yy} g_{zz}] = [2.00906 2.00687 2.00300]; [16] A = [A_{xx} A_{yy} A_{zz}] = [13 13 96] MHz.
A superposition of a mobile component in the fast motion regime and a less mobile component in the slow motion regime was used. The fraction of the mobile component was smaller than 1 %.

4.2.4 Second-moment analysis

Since the line width of the EPR spectra depends amongst other factors also on the spin-spin interaction, the spectral second moment was used to quantify this interaction. In all experiments, a sample of a monomer, with a spectrum $S_M(B)$ was compared to a sample in which the spin-spin

interaction is present $S_D(B)$. The difference of spectral second moments $<\Delta B^2>$ was calculated according to the following equation: [17]

$$<\Delta\Delta B^2> = \frac{\int (B - B_{FD})^2 S_D(B) dB}{\int S_D(B) dB} - \frac{\int (B - B_{FM})^2 S_M(B) dB}{\int S_M(B) dB} \quad (1)$$

where $S_D(B)$ is the absorption spectrum broadened due to dipolar spin-spin interaction, $S_M(B)$ is the absorption spectrum without spin-spin-interaction, B_{FD}, B_{FM} and B are the first spectral moments and the magnetic field, respectively. Second moments are defined as $<\Delta B_M^2>$ for the non-interacting and $<\Delta B_D^2>$ for the interacting case.
The absorption EPR spectra were baseline corrected using Xepr software (Bruker Biospin, Rheinstetten, Germany) and the first and second moment were calculated numerically using MatLab (MathWorks, MA, USA).

4.3 Results

The EPR spectra of SL-WALP were measured at different temperatures in the presence of membranes (multi-lamellar vesicles) composed of DOPC or DPPC lipids.
Label efficiency. The labeling degree and basic characteristics of the WALP samples are best judged by room-temperature EPR. In these spectra, spin-labeled WALP has a characteristic line-shape that can be identified in the simulation as a broadened spectrum (Fig. 2: 308 K) and a rotation correlation time τ_R = 2.3 ns (Table 2). A quantitative comparison of the EPR signal intensity to a reference sample with known spin concentration revealed that more than 90% of the peptides are spin labeled, in agreement with the mass-spectrometry results (see Material and Methods).
Additionally, a fast motion component is required in the simulation, which is attributed to a fraction of free MTSL. In all cases, this fraction is below 1 %, showing that free MTSL is efficiently removed by the post-labeling purification procedure.

Table 2

Parameters from the simulation (τ_c, ΔB) and the second moment analysis ($<\Delta B^2>$, $<\Delta\Delta B^2>$) of pure SL-WALP and dd-SL-WALP in DOPC and DPPC

sample	temperature (K)	correlation time τ_c (ns) [a]	line width ΔB (T) [b]	second moment $<\Delta B^2>$ (T^2) [c,d]	broadening $<\Delta\Delta B^2>$ (T^2)
dd-SL-WALP DPPC	120	---	---	$2.8*10^{-6}$	$4.5*10^{-6}$
SL-WALP DPPC	120	---	---	$7.3*10^{-6}$	
dd-SL-WALP DPPC	290	5.8	$4.2*10^{-4}$	$2.6*10^{-6}$	$2.0*10^{-6}$
SL-WALP DPPC	290	5.8	$8.1*10^{-4}$	$4.6*10^{-6}$	
dd-SL-WALP DPPC	308	2.3	$1.2*10^{-4}$	$2.1*10^{-6}$	$1.1*10^{-6}$
SL-WALP DPPC	308	2.3	$2.8*10^{-4}$	$3.2*10^{-6}$	
dd-SL-WALP DPPC	333	1.2	$1.1*10^{-4}$	$2.3*10^{-6}$	$0.1*10^{-6}$
SL-WALP DPPC	333	1.2	$1.3*10^{-4}$	$2.4*10^{-6}$	
dd-SL-WALP DOPC	120	---	---	$2.8*10^{-6}$	$2.6*10^{-6}$
SL-WALP DOPC	120	---	---	$5.4*10^{-6}$	
dd-SL-WALP DOPC	240	---	---	$2.5*10^{-6}$	$0.8*10^{-6}$
SL-WALP DOPC	240	---	---	$3.3*10^{-6}$	
dd-SL-WALP DOPC	260	---	---	$2.1*10^{-6}$	$-0.1*10^{-6}$
SL-WALP DOPC	260	---	---	$2.0*10^{-6}$	
dd-SL-WALP DOPC	290	2.2	$1.1*10^{-4}$	$2.2*10^{-6}$	$0.2*10^{-6}$
SL-WALP DOPC	290	2.2	$1.8*10^{-4}$	$2.4*10^{-6}$	

[a] The rotation correlation time (τ_c) error is $\pm$ 0.1 ns

[b] The intrinsic line width (ΔB) error is $\pm\ 0.1*10^{-4}$ T

[c] The subscript i indicates the second moment for the spectra with and without spin-spin interaction

[d] The second moment $<\Delta B^2>$ error is $\pm\ 0.2*10^{-6}$ T^2

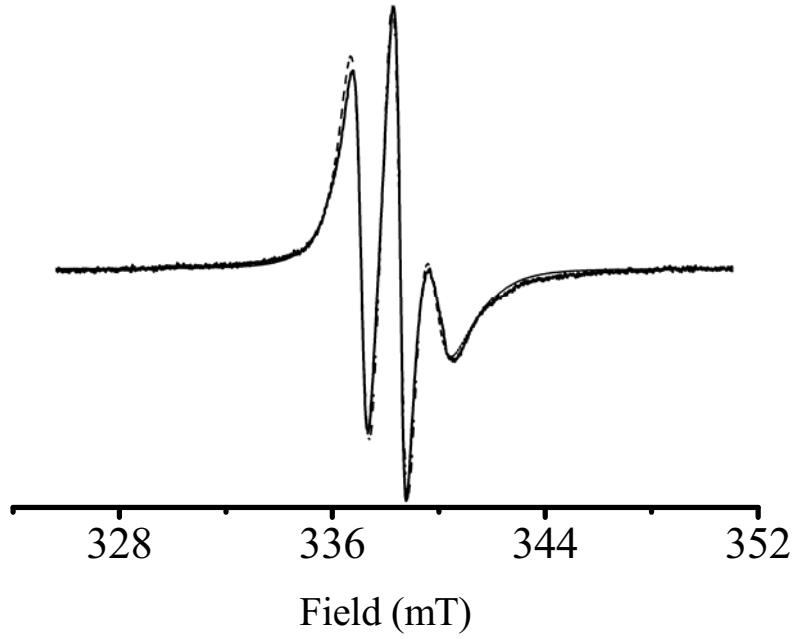

Fig. 2: The cw EPR spectrum of spin-labeled WALP at 308 K and its simulation. Pure SL-WALP in DPPC (solid line); simulation (dashed line). (For the simulation parameters see "Materials and methods" and Table 1).

EPR at 120 K. Fig. 3 shows EPR frozen solution spectra (T =120 K) of pure SL-WALP in DOPC and DPPC and of diamagnetically diluted (dd) SL-WALP in DPPC. The spectrum of dd-SL-WALP in DOPC, not shown in the picture, is identical to the one in DPPC. The phase-transition temperature (T_m) between the liquid-crystalline phase (higher temperature) and the gel phase (lower temperature), of DOPC and DPPC is 253 K and 314 K respectively, 18 so at the measurement temperature of 120 K both lipids are in the gel phase. Both the dd-SL-WALP and SL-WALP spectra can be well simulated as immobilized powder spectra. From the dd-SL-WALP spectra the hyperfine tensor (A) and the g-tensor (G) parameters are obtained. The spectra are normalized to the same number of spins, therefore, the smaller amplitude of the spectra of SL-WALP in DPPC and in DOPC relative to the spectrum of dd-SL-WALP reflects the broadening of the spectra of the SL-WALP samples.

For SL-WALP in DPPC, the spectra are more broadened than those of the SL-WALP in DOPC. To test the conditions for diamagnetic dilution, a sample composed of 10% SL-WALP and 90% WALP (10% dd-SL-WALP) was compared to a mixture of 20% SL-WALP with 80% WALP in DPPC, (20% dd-SL-WALP).

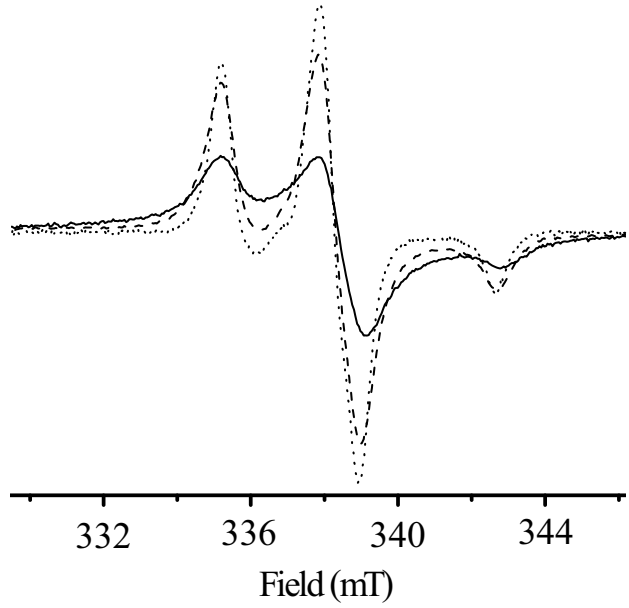

Fig. 3: The cw EPR spectra of spin-labeled WALP at 120 K. Pure SL-WALP in DOPC (dashed line); experimental conditions: microwave (mw) attenuation: 29 dB; total acquisition time: 14 min. Pure SL-WALP in DPPC (solid line); mw attenuation: 23 dB; total measurement time: 28 min; and dd-SL-WALP (10%) in DPPC (dotted line); mw attenuation: 38 dB; total measurement time: 56 min. All spectra, P/L: 1/100. Spectra are normalized to the same number of spins. (For the remaining experimental parameters see "Materials and methods").

The spectra of both samples were identical, showing that spin-spin interactions do not contribute to the lineshape for 10% and 20% dd-WALP. In the following, both 10% and 20% SL-WALP are referred to as dd-SL-WALP.

The width of the spectra is given by the second moment of the spectra ($<\Delta B_i^2>$), and the broadening is expressed by $<\Delta B_D^2> - <\Delta B_M^2> = <\Delta\Delta B^2>$, where $<\Delta B_D^2>$ is the second moment of the SL-WALP sample, $<\Delta B_M^2>$ is the second moment of the dd-SL-WALP sample and $<\Delta\Delta B^2>$ the difference in the second moment. The second moments of the EPR spectra are given in Table 2. Positive $<\Delta\Delta B^2>$ values reveal broadening, and in the following positive $<\Delta\Delta B^2>$ values will be referred as broadening. The $<\Delta\Delta B^2>$ value of SL-WALP in DPPC is bigger than the value found for the SL-WALP in DOPC. This indicates that at 120 K WALP has a higher degree of aggregation in DPPC than in DOPC (see Discussion). Different P/L ratios of SL-WALP in DOPC and DPPC were measured. For DPPC, the same line shape was observed for P/L ratios of 1/30 and 1/100, for DOPC the line was a little wider for the P/L ratio of 1/30, without, however, resulting in a significant increase in $<\Delta\Delta B^2>$. This indicates that the P/L ratios in that range do not significantly affect the spin-spin interaction.

To investigate whether there is a preferred arrangement, i.e. parallel or anti-parallel, of the WALP molecules in the membrane, a set of experiments was performed with WALP spin labeled at the N- or the C-terminal positions (SL-N-WALP and SL-C-WALP). The $<\Delta\Delta B^2>$ values for SL-N- and SL-C-WALP in DPPC are smaller than those for SL-WALP in the same membrane environment, due to increased motional freedom of the label, yet the broadening remains significant (Table 3). Spectra of SL-N-WALP and SL-C-WALP, mixed in the same sample were indistinguishable from the spectra of SL-N-WALP and SL-C-WALP measured separately, suggesting that there is no preferred alignment in DPPC at 120 K (see Discussion). For DOPC, the SL-N- and SL-C-WALP spectra have such small $<\Delta\Delta B^2>$ values that it was not possible to analyze the difference between pure SL-N-WALP resp. SL-C-WALP and the mixed sample.

Table 3
Parameters form second moment analysis ($<\Delta B^2>$, $<\Delta\Delta B^2>$) of pure SL-C-WALP and SL-C/N-WALP and dd-SL-C-WALP and dd-SL-C/N-WALP in DPPC.

sample	temperature (K)	second moment $<\Delta B^2>$ (T^2) [a b]	broadening $<\Delta\Delta B^2>$ (T^2)
dd-SL-C-WALP DPPC	120	$4.0*10^{-6}$	$1.1*10^{-6}$
SL-C-WALP DPPC	120	$5.1*10^{-6}$	
dd-SL-N/C-WALP DPPC	120	$4.0*10^{-6}$	$1.1*10^{-6}$
SL-N/C-WALP DPPC	120	$5.1*10^{-6}$	

[a] The subscript i indicates the second moment for the spectra with and without spin-spin interaction
[b] The second moment $<\Delta B^2>$ error is $\pm 0.2*10^{-6}$ T^2

EPR at temperatures higher than 120 K. Below 240 K, both DPPC and DOPC are in the gel phase, and at 120 K, the spectra of dd-SL-WALP revealed complete immobilization. At 240 K DOPC is still in the gel-phase, but the line-shape of dd-SL-WALP (Fig. 4a) deviates from that of the immobilized spin label towards a more mobile form. The line-narrowing expected for the higher mobility is also reflected in the trend towards smaller $<\Delta B^2>$ values (Table 2). Also, the $<\Delta\Delta B^2>$ value is reduced relative to the value at 120 K (for interpretation, see Discussion). At 260 K, above the T_m of DOPC, where the lipids are in the liquid-crystalline phase, the spectra of dd-SL-WALP and SL-WALP are indistinguishable (Fig. 4b). The second moment $<\Delta B^2>$ of dd-SL-WALP is again reduced relative to the value of 240 K, and it is identical within experimental error to the value of SL-WALP, i.e. $<\Delta\Delta B^2>$ vanishes (Table 2). Also, at room temperature (290 K), no significant broadening was observed (Table 2).

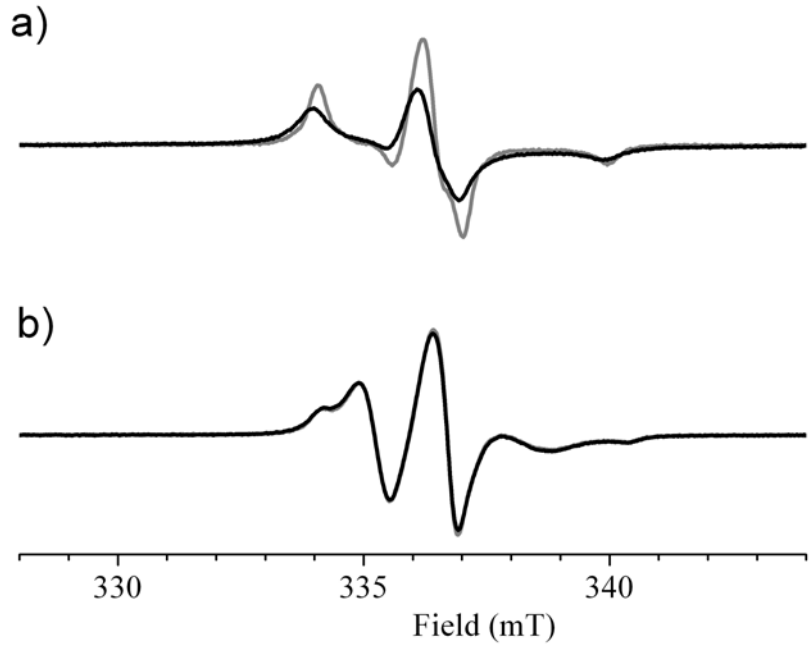

Fig. 4: The cw EPR spectra of spin-labeled WALP in DOPC, below and above T_m. (a) The pure SL-WALP spectrum at 240K (black), the dd-SL-WALP (20%) spectrum at 240 K (grey). (b) The SL-WALP spectrum at 260 K (black). The dd-SL-WALP (20%) spectrum at 260 K (grey). For all spectra, P/L ratio: 1/100. Spectra are normalized to the same number of spins. (For the remaining experimental parameters see "Materials and methods").

The T_m of DPPC is higher than that of DOPC, therefore, the respective experiments for DPPC are performed at a higher temperature. The Fig. 5a and 5b show EPR of pure and dd-SL-WALP in DPPC, at 290 K and at 308 K, i.e. below T_m. At both temperatures, the SL-WALP is significantly broadened with respect to the diamagnetically diluted one. The spectra were simulated using standard liquid solution parameters, resulting in rotation correlation times τ_R in the ns-time regime. Spectra of SL-WALP and dd-SL-WALP under identical membrane conditions could be simulated with identical values for τ_R but a larger ΔB for the

pure SL-WALP (Table 2). Fig. 5c shows EPR liquid-solution spectra of pure and diamagnetically diluted SL-WALP in DPPC at 333 K. At this temperature, which is above the T_m, DPPC is in the liquid-crystalline phase. The spectrum of SL- WALP (Fig. 5c) has a lower intensity, suggesting that the spectrum is slightly broader than the one of dd-SL-WALP. However, this broadening is not sufficient to lead to a $<\Delta\Delta B^2>$ value that is significantly above zero (Table 2).

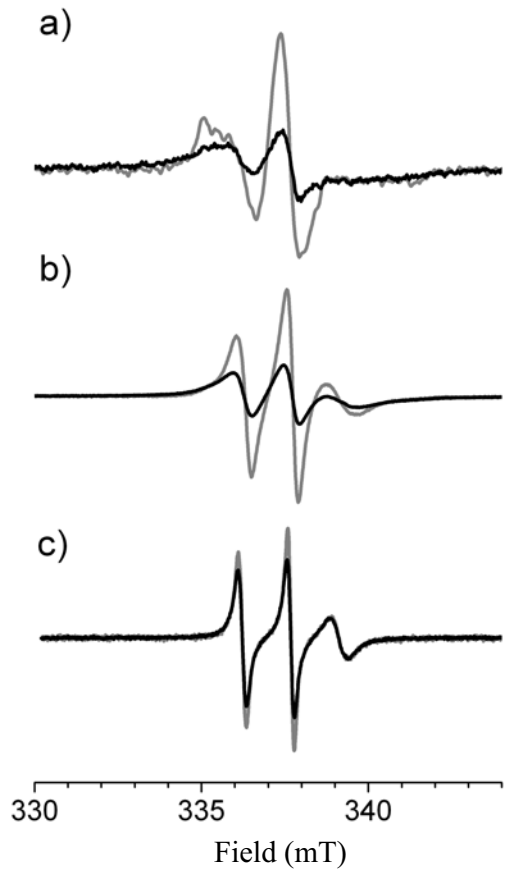

Fig. 5: The cw EPR spectra of spin-labeled WALP in DPPC below and above T_m. Pure SL-WALP (black) and dd-SL-WALP (20 %, grey) at a) T=290 K, b) T=308 K, and c) T=333 K. P/L ratio: 1/100. Spectra are normalized to the same number of spins. (For the remaining experimental parameters see "Materials and methods").

Model for the spin-spin interaction In order to interpret the measured $<\Delta\Delta B^2>$ values of the samples at 120 K, the dipolar interaction was calculated for model aggregates. For a spin pair, the $<\Delta\Delta B^2>$ value is related to the distance as

$$\left\langle \Delta\Delta B^2 \right\rangle = p\frac{1}{R^6} \tag{2}$$

where R is the spin-spin distance and $p \approx 1.56 \cdot 10^{-60} T^2 m^6$. [17] Aggregates of more than two spins are modeled taking all pair interactions into account

$$\left\langle \Delta\Delta B^2 \right\rangle = \sum_i \left\langle \Delta\Delta B_i^{\,2} \right\rangle = p\sum_i \frac{1}{R_i^6} \ , \tag{3}$$

where the second moments of each two-particle interaction are added. [19] The membrane is assumed to be two-dimensional, and the dipolar broadening due to line aggregates as well as two-dimensional cluster aggregates was calculated. The aggregates are modeled as having a fixed spin-spin distance R between nearest neighbors. To illustrate the procedure, a linear trimer is discussed. In this case, the central spin has two neighbors at a distance R and the spins at the ends of the aggregate have one neighbor at the distance R and one neighbor at the distance 2R, resulting in the second moment

$$\left\langle \Delta\Delta B^2 \right\rangle = p\left(\frac{1}{3}\frac{2}{R^6} + \frac{2}{3}\left(\frac{1}{R^6} + \frac{1}{(2R)^6} \right) \right). \tag{4}$$

Similarly, linear aggregates of any size up to the infinitely long line aggregate ($\left\langle \Delta\Delta B^2 \right\rangle = \frac{2\pi^6}{945}\frac{p}{R^6}$) as well as cluster aggregates can be calculated. The inter-spin distance R in the aggregates is estimated from a model in which the transmembrane helix of one WALP touches the surface of the adjacent WALP. Using a helix diameter of 1 nm, a distance between spin labels of 1 nm results, if the linker joining the spin label to the WALP-peptide backbone has the same orientation in both

peptides. Since the linker length of MTSL in the extended conformation is 0.5 nm and there is no information on the rotational orientation of the WALP-helices in the membrane, we also investigated the effect of R on the broadening.

As a reference, also the second moment of non-aggregated, i.e., randomly distributed spins in the membrane is needed. The number of spins *N(r)dr* at a distance between *r* and *r* + *dr* from a spin is

$$N(r)dr = c2\pi r dr\,, \tag{5}$$

with c, the density of spins in the membrane. Introducing R_0, the distance of closest approach, a broadening of

$$\left\langle \Delta\Delta B^2 \right\rangle = p\int_{R_0}^{\infty} N(r)\frac{1}{r^6}dr = \frac{1}{2}\pi cp\frac{1}{R_0{}^4} \tag{6}$$

results. The distance of the closest approach corresponds to the helix diameter, i.e. R = R_0. To obtain an estimate of the magnitude of this broadening, the density c is calculated from the area of the headgroup of the lipids of 82 $Å^2$ and 52.3 $Å^2$ for DOPC and DPPC, respectively. [20,21] For a peptide/lipid ratio of 1/100, corresponding to an area of 50 lipid heads in the bilayer per spin, a density of c = $(41\ nm^2)^{-1}$ for DOPC and $(26\ nm^2)^{-1}$ for DPPC results. Only a rough estimate of this factor will be needed in the following discussion.

In Fig. 6, the results of the calculated $<\Delta\Delta B^2>$ values are plotted as a function of R. Broadening obtained from model calculations of linear clusters containing 2, 3, 4, 5, or an infinite number of spin-labeled peptides as well as clusters of 3, 4, and 7 peptides is shown. In order to calculate the broadening due to a random distribution for Fig. 6 an averaged density of $(35\ nm^2)^{-1}$ was used. Linear aggregates yield smaller degrees of broadening than cluster aggregates, and, due to the r^{-6} dependence of the broadening, short distances dominate, such that, for example, the infinitely long line aggregate has a broadening that is close to the trimeric cluster aggregate.

In Fig. 6, also the experimental $<\Delta\Delta B^2>$ parameters are shown. Note that a direct comparison is only straightforward for the measurements at 120 K. For higher temperatures (partial) averaging can reduce the

broadening, as discussed below. The slight deviation of the absolute values due to incomplete labeling has been neglected.
In the following, we will analyze the experimental results and compare them to the calculation to construct a picture of WALP interaction in DOPC and DPPC.

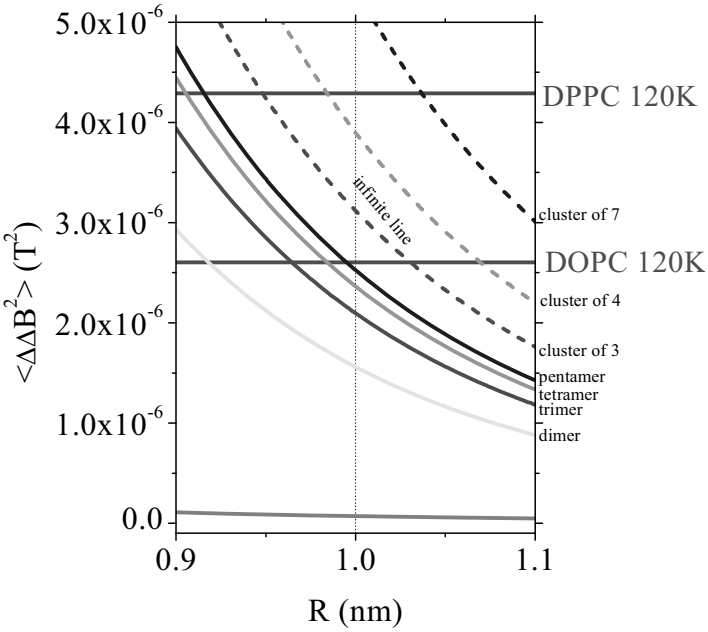

Fig. 6: The second moment (spectral broadening owing to dipolar interaction) as a function of the nearest neighbor spin distance R for different model geometries derived from calculations. Linear aggregates are shown as solid lines, in order of increasing broadening containing 2 (dimer), 3 (trimer), 4 (tetramer), 5 (pentamer), or an infinite number of spins (infinite line). Dashed lines correspond to 2D clusters containing (again in order of increasing broadening) 3, 4, or 7 molecules, respectively. The broadening for 2D randomly distributed spins as a function of closest approach (R_0) - see text - is visualized by the grey solid line. The experimentally obtained broadening values for spin labeled WALP in model membranes (P/L=1/100) at 120 K are depicted as horizontal lines: DPPC and DOPC.

4.4 Discussion

The goal of this study was to use EPR to investigate whether certain membrane conditions promote peptide-peptide aggregation. In the following we interpret the EPR spectra and develop a model for the arrangement of the peptides in the membrane.

In the gel phase of the lipids, at 120 K, the spin labels are immobilized, and the close approach of the spin labels in the pure SL-WALP causes line broadening due to the dipole-dipole interaction. The broadening is more pronounced for SL-WALP in DPPC than in DOPC, showing that the dipolar interaction is stronger for SL-WALP in DPPC than in DOPC. Model calculations (see Results) relate this broadening, expressed as the difference in second moments $<\Delta\Delta B^2>$, to the interaction of spin labels in different types of aggregates, namely cluster aggregates (Fig. 1b) and line aggregates (Fig. 1c). Given the disordered state of the membrane, such models can only be approximate, but we show that they can be used to classify the states of aggregates in a semi-quantitative way. Fig. 6 shows the results of the calculations together with the experimental values (olive and red horizontal lines). The broadening of the EPR spectra of SL-WALP in DOPC at 120 K is comparable to that of a linear aggregate containing five molecules for $R \geq 1$ nm. For SL-WALP in DPPC, $<\Delta\Delta B^2>$ is larger and at $R \geq 0.95$ nm it is in the cluster region of the diagram, close to the tetrameric cluster aggregate. This suggests that, in the gel phase of DPPC, WALP aggregates are likely of the cluster type, whereas in DOPC the aggregates are more likely to be line-type aggregates.

Line-type and cluster aggregates should also have distinct characteristics when C-and N-terminally labelled peptides are compared. For line aggregates with a strictly antiparallel (parallel) arrangement, the mixed sample should have a smaller (larger) interspin distance than the individual SL-C or SL-N-WALP samples, resulting in a larger (smaller) $<\Delta\Delta B^2>$. For cluster aggregates only very specific configurations can be envisaged that would have a strictly antiparallel arrangement of the peptides, making random orientations more likely.

For WALP in DPPC, no difference in broadening between SL-N and SL-C-WALP measured individually or combined in one sample was observed (see Results). This argues for either a line aggregate with random arrangements of the C- and N-termini of WALP, i.e., neither

strictly parallel or antiparallel, or for a cluster type aggregate. The latter form would be favoured also from the amount of broadening. In DOPC, the broadening of the N- and C-terminal labelled WALP was too small to be detected. For the pure SL-C- or N-WALP samples we attribute this to the long distance between the spin labels in our constructs in the anti-parallel orientation. For the SL-C- and N-WALP mixed samples, the long distance and the overall smaller broadening in the line-aggregates, compared to the cluster aggregates, makes the broadening too small to be detected. Taking all into account, the simplest interpretation of the data so far would be cluster aggregates for WALP in the gel phase of DPPC and line aggregates for WALP in the gel phase of DOPC.
Before doing the same analysis for the liquid-crystalline phase of the lipids, first the effect of higher temperatures on the spectra has to be discussed. Above 120 K and particularly at 240 K and above, the mobility of SL-WALP in the membrane increases, and this could (partially) average the dipolar interaction. Such an averaging can only be excluded, if the correlation time of the interspin vector is long enough to fulfill the following condition: [19]

$$\tau_c \left(\left\langle \Delta\omega_0^2 \right\rangle \right)^{\frac{1}{2}} = \tau_c \left(4\pi^2 (2.8*10^{10} \frac{Hz}{T})^2 \left\langle \Delta\Delta B_0^2 \right\rangle \right)^{\frac{1}{2}} >> 1 \qquad (7)$$

With the broadening $< \Delta\Delta B^2 >$ obtained from the frozen solution data (Table 2 and 3) this condition (Eq. 7) can be rewritten as

$$\tau_c >> \tau_c^* \ , \qquad (8)$$

with the critical correlation time τ_c^*. Assuming that the correlation time of the interspin vector corresponds to the spin-label rotational correlation time, for temperatures above 240 K one obtains the corresponding ratio to be in the range of $\frac{\tau_c}{\tau_c^*} \approx 0.4 \, to \, 1.7$, i.e., far from the requirement stated in Eq. 8. Therefore the broadening could be reduced by motional narrowing.
For WALP at 290 K and 308 K in DPPC, the membrane is still in the gel phase but the spectra of dd-SL-WALP are narrowed relative to those at

120 K, revealing the increased mobility of the spin label under these conditions. Also, $<\Delta\Delta B^2>$ decreases, but it remains significantly larger than the $<\Delta\Delta B^2>$ expected for a random distribution of isolated spins in the membrane, a clear indication of aggregation. The reduction in $<\Delta\Delta B^2>$ could be caused by (partial) averaging of the dipolar interaction and/or a conversion of cluster aggregates into smaller aggregates or line-type aggregates. The difficulty to quantify the contribution of both factors to the reduction in $<\Delta\Delta B^2>$ makes it impossible to discriminate between both effects and to determine a possible change in aggregate size or shape.

In the liquid-crystalline state (T = 333 K), $<\Delta\Delta B^2>$ is much smaller than at 308 K, while the experimentally determined τ_c values are only slightly smaller than those at 308 K, where the membrane is in the gel state. The decreased broadening at temperatures above the phase transition is still significant even if one would assume a linear decrease of $(<\Delta\Delta B^2>)^{1/2}$ with τ_c. Hence, it is plausible that the dipolar interaction is not only averaged but indeed smaller, which would suggest less or no aggregation in the liquid-crystalline state of the membrane. This hypothesis is supported by the fact that the broadening increases proportionally to the peptide lipid ratio in a range between 1/100 to 1/30 (data not shown) as expected for randomly distributed spins (eq 6). For SL-WALP in DOPC $<\Delta\Delta B^2>$ follows a similar pattern as in DPPC, suggesting that also in DOPC there is aggregation below, but not above T_m. However, in DPPC the tendency to aggregate below T_m seems larger than for DOPC.

If aggregation occurs only in the gel phase, upon cooling the samples through T_m to create the gel-phase, the peptides, which are randomly distributed in the membrane in the liquid-crystalline phase, must diffuse towards each other when the membrane enters the gel phase. This requires that the peptide diffusion in the membrane must be faster than cooling through the phase transition, a condition obviously met in the cooling protocol used in the present study.

In summary, we conclude that, at 120 K, WALP aggregates in the gel phase of DPPC most likely as clusters and in DOPC as line aggregates, but not in the liquid crystalline phase of the lipids.

Previously, aggregation of WALP in the gel-phase of DPPC had been observed by atomic force microscopy (AFM). Line-type depressions were observed by AFM [1,7,8] and interpreted as linear aggregates of WALP. Striated domains are made up of parallel line depressions in

which the lines are separated by 8 nm. These results suggest that the EPR parameters should only reveal linear aggregates, as the distance to an adjacent line in striated domains is too large to cause broadening according to the model used for the two-dimensional aggregates. The line aggregate model would allow for close contact of maximally four WALP peptides at the bifurcation points of line depressions, but such points should only represent a minority of the sites [1]. Fluorescence studies of the same system revealed antiparallel aggregates that, in the light of the AFM results, may also be interpreted as line aggregates. [1,9]

An obvious difference between AFM and fluorescence experiments on the one hand and the EPR experiments on the other hand is that the latter experiments are performed at significantly lower temperatures (120 K for EPR, AFM and fluorescence not below 297 K). If, upon lowering the temperature, lipid-lipid interactions become stronger, the lipids could force the peptides into cluster type aggregates as that would decrease the lipid-peptide interaction surface. This would require the peptides to give up the more favourable antiparallel arrangement possible only in the line aggregates. The smaller $<\Delta\Delta B^2>$ values at higher temperatures are consistent with a reduction in cluster size and conversion to line aggregates, but the increased mobility of the peptides at higher temperatures makes it impossible to determine that factor.

The AFM results also showed that aggregate signatures disappear upon heating the DPPC sample above the phase transition into the liquid crystalline phase [1]. Similarly, the yield of excimers decreases sharply upon heating above T_m, showing that aggregates that were present in the gel-phase, i.e. below T_m, break up in the liquid-crystalline phase.[1] The remaining excimer contribution at higher temperatures, in the order of 5 %, is likely to be too small to be detected by EPR, because in the liquid-crystalline phase partial averaging of the dipolar interaction interferes. To estimate the minimum amount of aggregated SL-WALP that could be detected in the liquid-crystalline phase under these conditions is difficult, but a minimum of 30 % seems likely. This would make it impossible to detect the amount of aggregation found in the fluorescence studies.

Our study provides the first experimental data about aggregation of WALP in the gel phase of DOPC, and our data suggests linear aggregates at 120 K. In the liquid-crystalline phase, excimer formation of WALP, suggesting dimers or higher aggregates, had been found for

P/L ratios above 1/50, [9] but also smaller amounts of aggregates were observed for P/L ratios 1/100. [1] But again, the yield of excimers found by optical methods was small (around 5 %) [1] and thus below the detection limit of EPR in the liquid crystalline phase of the membrane.
The emerging picture of aggregation of WALP in the two membranes is the following: Previously, aggregation of WALP in the gel phase of DPPC was found by AFM, optical spectroscopy and NMR [1,7]. Our observations of SL-WALP at 120 K agree with these results, although our interpretation suggests cluster rather than line aggregates. We propose that at the temperature of the EPR experiments cluster aggregates prevail, because lipid-lipid interactions become stronger at lower temperatures. Even though the peptide-peptide interaction seems to favour an antiparallel arrangement of the peptides, [9,14] this energy gain could be offset by the increasingly unfavourable lipid-peptide interaction. Under these circumstances, cluster aggregates that minimize the lipid-peptide interface could be the optimal solution.
Aggregation in the gel phase of DOPC had not been reported before. The aggregation of the peptides in DPPC was attributed to the balance of lipid-lipid and lipid-peptide interactions in the gel phase of the saturated lipid DPPC, particularly, by the increased ordering of the lipid chains in the vicinity of WALP found by NMR. [1] Aggregation in the gel phase of DOPC indicates that the lipid order in the gel phase is sufficient to induce aggregation of WALP, even though this ordering is expected to be compromised by the unsaturated lipid chains of DOPC, or, in other words that the gel phase is more important than the precise structure of the lipid in the vicinity of WALP.

4.5 Conclusion

The approach to combine EPR line broadening, diamagnetic dilution and model calculations provides information on aggregate shape and, in certain cases, also the size of the aggregates. This approach should be applicable to a wide range of membrane conditions.
The higher degree of order of the lipid chains in the gel phase seems to be a major factor in promoting aggregation because both the saturated lipid DPPC and the unsaturated lipid DOPC promote WALP aggregation in that phase. However, the degree of saturation of the lipids seems to

affect the type of aggregation and our analysis suggests cluster aggregates in DPPC and line aggregates in DOPC. The strength of lipid-peptide interactions may also depend on temperature. In DPPC, EPR at 120 K indicates cluster aggregates, whereas AFM at 297 K reveals line aggregates.
The degree of aggregation must be significantly smaller in the liquid-crystalline phase of both lipids, but experimental limitations in the fluid, mobile regime of the membrane limit the sensitivity and uniqueness of the answers obtained. Such limitations can, in principle, be overcome by a quantitative analysis of the peptide mobility in the membrane.
The EPR approach presented is suitable to investigate the state of peptides in membrane. It should be applicable to a wide range of membrane conditions. We demonstrate it for the gel-phase of two lipids. In view of the occurrence of gel-phase like states in biological membranes, this presents a relevant step ahead in the study of lipid-peptide interaction.

Acknowledgments

I would like to thank dr. Malte Drescher for his active role in this project. He performed the EPR measurements of part of the samples and developed the aggregation model, dr. prof. Antoinette Killian, Andrea Holt for the help in the preparation of the lipid samples and the useful suggestions and Tania Meijneke who prepared the peptide samples.

Reference list

1. Sparr, E.; Ganchev, D. N.; Snel, M. M. E.; Ridder, A. N. J. A.; Kroon-Batenburg, L. M. J.; Chupin, V.; Rijkers, D. T. S.; Killian, J. A.; de Kruijff, B. *Biochemistry* **2005,** *44*, 2-10.
2. Killian, J. A.; Nyholm, T. K. M. *Current Opinion in Structural Biology* **2006,** *16*, 473-479.
3. Ozdirekcan, S.; Etchebest, C.; Killian, J. A.; Fuchs, P. F. J. *Journal of the American Chemical Society* **2007,** *129*, 15174-15181.
4. Lemaitre, V.; de Planque, M. R. R.; Howes, A. P.; Smith, M. E.; Dupree, R.; Watts, A. *Journal of the American Chemical Society* **2004,** *126*, 15320-15321.
5. Holt, A.; de Almeida, R. F. M.; Nyholm, T. K. M.; Loura, L. M. S.; Daily, A. E.; Staffhorst, R. W. H. M.; Rijkers, D. T. S.; Koeppe, R. E.; Prieto, M.; Killian, J. A. *Biochemistry* **2008,** *47*, 2638-2649.
6. Nielsen, R. D.; Che, K. P.; Gelb, M. H.; Robinson, B. H. *Journal of the American Chemical Society* **2005,** *127*, 6430-6442.
7. Rinia, H. A.; Kik, R. A.; Demel, R. A.; Snel, M. M. E.; Killian, J. A.; van der Eerden, J. P. J. M.; de Kruijff, B. *Biochemistry* **2000,** *39*, 5852-5858.
8. de Kruijff, B.; Killian, J. A.; Ganchev, D. N.; Rinia, H. A.; Sparr, E. *Biological Chemistry* **2006,** *387*, 235-241.
9. Sparr, E.; Ash, W. L.; Nazarov, P. V.; Rijkers, D. T. S.; Hemminga, M. A.; Tieleman, D. P.; Killian, J. A. *Journal of Biological Chemistry* **2005,** *280*, 39324-39331.
10. de Planque, M. R. R.; Greathouse, D. V.; Koeppe, R. E.; Schafer, H.; Marsh, D.; Killian, J. A. *Biochemistry* **1998,** *37*, 9333-9345.
11. Bashtovyy, D.; Marsh, D.; Hemminga, M. A.; Pali, T. *Protein Science* **2001,** *10*, 979-987.
12. Margittai, M.; Langen, R. *Amyloid, Prions, and Other Protein Aggregates, Pt C* **2006,** *413*, 122-139.
13. Der-Sarkissian, A.; Jao, C. C.; Chen, J.; Langen, R. *Journal of Biological Chemistry* **2003,** *278*, 37530-37535.
14. Yano, Y.; Matsuzaki, K. *Biochemistry* **2006,** *45*, 3370-3378.

15. Stoll, S.; Schweiger, A. *Journal of Magnetic Resonance* **2006,** *178*, 42-55.
16. Steigmiller, S.; Borsch, M.; Graber, P.; Huber, M. *Biochimica et Biophysica Acta-Bioenergetics* **2005,** *1708*, 143-153.
17. Steinhoff, H. J. *Frontiers in Bioscience* **2002,** *7*, C97-C110.
18. John Wiley & Sons *Lipid-Protein Interactions;* New York, 1982.
19. Abragam, A. *The Principles of Nuclear Magnetism;* Oxford University Press: Oxford, 1961.
20. Nagle, J. F.; Tristram-Nagle, S. *Biochimica et Biophysica Acta-Reviews on Biomembranes* **2000,** *1469*, 159-195.
21. Lis, L. J.; Mcalister, M.; Fuller, N.; Rand, R. P.; Parsegian, V. A. *Biophysical Journal* **1982,** *37*, 657-665.